Hindawi
Discrete Dynamics in Nature and Society
Volume 2024, Article ID 9912671, 17 pages
https://doi.org/10.1155/2024/9912671

Research Article

Dynamic Analysis of a Simple Cournot Duopoly Model Based on a Computed Cost

S. S. Askar and Ahmad M. Alshamrani

Department of Statistics and Operations Research, College of Science, King Saud University, P.O. Box 2455, Riyadh 11451, Saudi Arabia

Correspondence should be addressed to S. S. Askar; saskar@ksu.edu.sa

Received 25 February 2023; Revised 11 February 2024; Accepted 5 March 2024; Published 25 March 2024

Academic Editor: Youssef N. Raffoul

The paper is organized to study some mathematical properties and dynamics of a simple Cournot duopoly game based on a computed quadratic cost. The time evolution of this game is described by a two-dimensional noninvertible discrete time map using the bounded rationality mechanism. For this map, some dynamic characteristics such as multistability and synchronization are investigated. Its equilibrium points are obtained for the asymmetric case, and their conditions of stability are obtained. Our results investigate that the Nash equilibrium point may be unstable due to flip bifurcation and under certain parameter values, and Neimark–Sacker bifurcation is born after the period-4 cycle. Through some restrictions, the coordinate axes of the map construct an invariant manifold, and therefore, their dynamics can be analyzed by using a one-dimensional map. In the symmetric case, both firms behave identically, and this implies that the diagonal set forms an invariant manifold, and hence the synchronization phenomena take place. Furthermore, the global bifurcation of the map is confirmed through contact between critical curves and the boundaries of infeasible domains.

1. Introduction

In this paper, investigations on the dynamics of nonlinear economic games whose competing players adopt linear inverse demand and horizontal differentiation with computed quadratic cost function derived from the Cobb–Douglas utility function are studied. The time evolution of this game is expressed by a two-dimensional nonlinear discrete-time map using the bounded rationality. Literature has reported several analyses of such economic games which have attracted many researchers because of the complicated behaviors of these maps. In the current paper, we focus on a special type of those maps that are known as duopoly maps. The focus of this paper is on studying duopoly games with quantity setting, and for future studies, we urge interested readers and researchers to investigate the cases of Cournot–Bertrand mixed game and triopoly under the conditions imposed on the current game. The duopoly game has been characterized by a market possessing only two competing firms (or players) seeking the optimal quantities that maximize players' profits. After Cournot, the famous French economist, who introduced the first duopoly model with quantity setting as decision variables, many works have been raised to study the dynamics of such games. Analyzing the dynamics of such games has been dated to [1] who died last year after enriching literature with many useful books and papers. In 1950, the Nash equilibrium point explored by John Nash, a famous American mathematician, has been raised in the theory of equilibrium points in noncooperative games. The Nash equilibrium point represented the optimum output of a game in which no player has an incentive to deviate from their chosen strategy after considering an opponent's choice. Studying the dynamic characteristics of duopoly games requires first to calculate the Nash point and then studying its stability. In fact, one should highlight the theory of games as an important applied mathematics tool that has been adopted to analyze the interaction amongst players in such economic

games. Game theory has been used for investigating strategic interactions amongst decision-makers and rational competitors. It was extensively developed in the 1950s by many scholars and was explicitly applied to several fields such as social science, logic relations, computer science, biology, and economics' models. Recently, it has been applied to economic models for studying the dynamic competition amongst competing firms. However, static equilibrium analysis of such games is limited and has not given valuable information on the time evolution of such games, although it has been studied by many researchers (see, for example, [2]). Dynamic studies give more valuable information on the stability/instability of Nash equilibrium, future predictions of the game's behavior, types of bifurcations by which the Nash point may lose its stability, and the topological structure of the phase plane describing the dynamics around the Nash equilibrium point. In literature, it has been reported that Rand [3] was the first person who analyzed some of these dynamic characteristics.

Literature has reported many works that have analyzed the dynamic characteristics of duopoly games. These dynamic characteristics have included bifurcation types such as flip and Neimark–Sacker, some attracting sets and chaotic attractors whose basin of attractions are represented by peculiar shapes, and synchronization and multistability phenomena. Moreover, adopting specific inverse demand functions requires using specific types of utility consumer preferences. One of the most important utilities in literature is known as the Cobb–Douglas utility which was used in several studies in the literature and is adopted in the current work. The reason is that the Cobb–Douglas utility represents a production function and has been widely used to represent the technological relationship between the inputs and production outputs. There are other utility functions that have been reported in the literature and used in such games, for example, constant elasticity of substitution (CES) and Singh and Vives utility. Interested readers on the properties of these utilities are advised to check references [4–10].

The complexity behind duopoly models and their dynamic characteristics reveal interesting information on game's evolution and its future predictions. Such interesting results on the complexity have been raised in the literature and opened new routes for investigations. Here, we report some related works and results from the literature. For instance, a Cournot duopoly game that is known as a mixed game (in such a game, the two decision variables are represented by quantity and price) has been analyzed in [11]. Other related works on duopoly and triopoly in which competing players or firms have sought optimality of production have been introduced and analyzed in [12–14]. In [15], a Cournot duopoly game with rational competing players adopting the bounded rationality mechanism and seeking the maximization of relative profits has been studied. Based on a theoretical framework, a mixed-type game has been formalized and analyzed in [8]. In [16], another mixed-type game has been introduced and studied by Naimzada et al. based on a two-dimensional discrete nonlinear map. They focused on analyzing the dynamics of Nash equilibrium and its instability through two different types of bifurcations. On the other hand, studying the complex dynamic characteristics of such a game requires building a map which is used to describe the time evolution of the game. From an economic perspective, this map is a tool by which firms can update their productions. Forming such maps depends on some adjustment rules. Amongst those rules, literature has extensively reported the famous one which is known as the bounded rationality approach. Many duopoly games have been deeply used this approach for the process of modelling the discrete maps used to represent the time evolutions of these games. This approach is called a gradient rule as it depends on the marginal profits of competing firms. It requires firms to perform an estimation for their marginal profits to see whether they are increased or decreased, and consequently, they may update their outputs next time step. Besides this approach, there are other mechanisms that have been adopted in the modelling process such as the tit-for-tat rule and local monopolistic approximation mechanism [17–27]. Other recent studies on the dynamics of such games have been recently reported in the literature [28–32]. Recent studies on the complicated dynamics of such games have been reported in literature [33–40]. In addition, the case of Cournot–Bertrand on where decision variables are quantity and price has been recently studied in [41].

In literature, many cost functions have been assumed to be linear or nonlinear, and in this manuscript, we introduce a computed quadratic cost function that is used for constructing our game's model. Our aim in this paper is to deepen the complex dynamic characteristics of the nonlinear Cournot duopoly game considering that competing players (or firms) operate with quadratic cost function (a case of decreasing returns-to-scale technology) with incomplete market information. This paper's game is presented by a two-dimensional (2D) nonlinear discrete dynamic map with four fixed points, three of which are boundary points while the fourth is an interior point representing a Nash equilibrium point. The complex dynamic behavior of the map is entirely analyzed based on the local and global investigations. These investigations show that the Nash equilibrium point can be destabilized through flip bifurcation, and under certain parameters, the values of Neimark–Sacker bifurcations are raised after the period-4 cycle. Furthermore, under some restrictions, synchronization and multistability are studied showing that the diagonal set in the phase plane forms an invariant manifold. In addition, the obtained results show that the game's map is noninvertible and its phase plane is formed by three zones that are Z_4, Z_2, and Z_0. Overall, the proposed game and its characteristics generalize some existing works in the literature [9, 10, 15].

In brief, the current paper consists of many sections. Section 2 introduces the market competition including the computation of cost and profit. In Section 3, the 2D game's map is formed and its characteristics such as critical curves and noninvertible properties are discussed. The map's fixed points and their stability are given in Section 4. In Section 5, the invariant manifold for the map is investigated through a one-dimensional map. In Section 6, the basin of attraction,

global analysis, and the case of independent firms are analyzed. Finally, the conclusion is presented in Section 7.

2. Market Competition

The market competition proposed in this paper consists of two firms labeled by F_1 and F_2. Both firms produce the quantities, q_1 and q_2, respectively. The market price is restricted to the following inverse demand functions (prices):

$$\begin{aligned} p_1 &= a - q_1 - dq_2, \\ p_2 &= a - q_2 - dq_1, \end{aligned} \tag{1}$$

where $a > 0$ denotes the maximum price in the market. The parameter d has an important influence on the dynamics of the competition. It denotes the degree of product differentiation or product substitution. If $d = 1$, one gets two identical inverse demand functions and hence homogeneous goods are provided to the market. If $d = 0$, the two prices are independent and the case of two monopolistic markets is raised. If $d \in [-1, 0)$, the complementarity between the two competing firms is obtained. We will discuss the analysis of competition in the case of substitutability on which $d \in [0, 1]$.

2.1. Computation of Cost and Profit Functions. In order to compute the quantities produced by the two firms, we recall the Cobb–Douglas [42] production function given by

$$q_i = E_i L^{\alpha} K^{1-\alpha}; \quad i = 1, 2, \tag{2}$$

where $E_i, i = 1, 2$ is a constant and refers to the total factor productivity, L denotes the total labor, and K is the total capital. α is a constant, and for simplicity, it is assumed to be 0.5. The total cost imposed by a firm can be computed as

$$\mathrm{TC} = wL + rK, \tag{3}$$

where w refers to the wage per unit of labor, while r denotes the rental price per unit of capital. Therefore, by substituting (2) in (3), the total cost for each firm takes the following form:

$$\mathrm{TC}_i = \frac{wq_i^2}{E_i^2 K} + rK; \quad i = 1, 2, \tag{4}$$

where the marginal cost is $\mathrm{MC}_i = (dTC_i/dq_i) = c_i q_i; i = 1, 2$ and $c_i = (2w/E_i^2 K) > 0$. Now, the profit is given by

$$\pi_i = \mathrm{TR}_i - \mathrm{TC}_i; \quad i = 1, 2, \tag{5}$$

where $\mathrm{TR}_i = p_i q_i$ is the total revenue. By using (1) and (4) in (5), the profits become

$$\begin{aligned} \pi_1 &= (a - q_1 - dq_2)q_1 - \frac{1}{2}c_1 q_1^2 - rK, \\ \pi_2 &= (a - q_2 - dq_1)q_2 - \frac{1}{2}c_2 q_2^2 - rK. \end{aligned} \tag{6}$$

3. The Competition Model

There are many mechanisms that have been used in the literature to build the discrete dynamic model describing such games. In this paper, the bounded rationality mechanism is adopted. It depends on the marginal profits of firms. The marginal profits $(\varphi_i = (\partial \pi_i / \partial q_i), i = 1, 2)$ then become as follows:

$$\begin{aligned} \varphi_1 &= a - (2 + c_1)q_1 - dq_2, \\ \varphi_2 &= a - (2 + c_2)q_2 - dq_1. \end{aligned} \tag{7}$$

In such games, firms watch their marginal profits $\varphi_i, i = 1, 2$ whether they are increased or decreased. If $\varphi_i > 0, i = 1, 2$, it means that firms are ready to increase their production in the next period of time, and otherwise, they decrease production or become naive. So, the updating of productions is described by the following mechanism:

$$q_i(t + 1) = q_i(t) + k_i(q_i)\varphi_i; \quad i = 1, 2. \tag{8}$$

Let us assume that $k_i(q_i) = k_i q_i; i = 1, 2$, where $k_i > 0, i = 1, 2$ is the parameter of speed of adjustment. It means that the relative production $(q_i(t + 1) - q_i(t)/q_i(t))$ is directly proportional to $\varphi_i; i = 1, 2$. By substituting (7) in (8), one gets the discrete map that is used to describe the evolution of the proposed game (or the game's repetition) as follows:

$$T(q_1, q_2): \begin{cases} q_1(t + 1) = q_1(t) + k_1 q_1(t)(a - (2 + c_1)q_1(t) - dq_2(t)), \\ q_2(t + 1) = q_2(t) + k_2 q_2(t)(a - (2 + c_2)q_2(t) - dq_1(t)), \end{cases} \tag{9}$$

where the time steps are denoted by the parameter $t = 0, 1, 2, \ldots$. Setting $\varphi_i = 0, i = 1, 2$ gives $q_i = (a/2 + c_i) - (d/2 + c_i)q_j; i, j = 1, 2; i \neq j$, which describes each firm's optimal (profit-maximizing) quantity of output. This can be thought of as describing a firm's best response to the other firm's level of output. Therefore, by using this symmetrical relationship between firms, we find the equilibrium quantity by fixing $q_1 = q_2$. The equilibrium levels make firms have no incentive to change their level of output.

3.1. Critical Curves and Noninvertible Property. The critical curves are used to describe the decision space and are responsible for dividing it into zones. The rank-1 of the critical curve is expressed by LC which forms a locus containing all

rank-1 preimages located on a set denoted by LC_{-1}. As one can see that map (9) is of class C^1 (continuously differentiable). This means that the set LC_{-1} can be defined as the locus of points such that the Jacobian determinant associated with it is vanished. So, LC_{-1} is given by

$$LC_{-1} \subseteq \left\{(q_1, q_2) \in \mathbb{R}^2 : \det\left(J\left(q_1, q_2\right)\right) = 0\right\}, \tag{10}$$

where $J(q_1, q_2)$ is the Jacobian matrix. Therefore, LC represents the rank-1 image of LC_{-1} under the map T, i.e., $LC = T(LC_{-1})$. For map (9), LC_{-1} is expressed by the following relation:

$$Aq_2^2 + Bq_1^2 + Cq_1q_2 - Dq_1 - Eq_2 + F = 0, \tag{11}$$

where

$$\begin{aligned} A &= 2d\left(2 + c_2\right), \\ B &= 2d\left(2 + c_1\right), \\ C &= 4\left(2 + c_1\right)\left(2 + c_2\right), \\ D &= a\left(4 + d + 2c_1\right)k_1k_2 + 2\left(2 + c_1\right)k_1 + dk_2, \\ E &= a\left(4 + d + 2c_2\right)k_1k_2 + 2\left(2 + c_2\right)k_2 + dk_1, \\ F &= 1 + a\left(k_1 + k_2\right) + a^2k_1k_2. \end{aligned} \tag{12}$$

Both LC and LC_{-1} are plotted at two different sets of parameter values in Figure 1. Figure 1(a) shows that LC_{-1} consists of two parts LC_{-1}^1 and LC_{-1}^2. Figure 1(b) shows also that LC consists of two parts LC^1 and LC^2. Both figures are plotted at the values of the parameters, $a = 1, c_1 = 0.2, c_2 = 0.3$, $k_1 = 0.5, k_2 = 0.4$, and $d = 0.2$. Figures 1(c) and 1(d) present those critical curves at the parameters values, $a = 2, c_1 = 0.4, c_2 = 0.3, k_1 = 1.25, k_2 = 1.26$, and $d = 0.5$. One can also see that map (9) is a noninvertible map since the two branches of the critical curve LC divide the decision space into three zones Z_4, Z_2, and Z_0. These zones possess the set of points with 0, 2, and 4 positive real number preimages. In order to declare that let us calculate the real rank-1 preimages for the origin point. By substituting $q_i(t + 1) = 0, i = 1, 2$ in map T and by solving the obtained algebraic system, one gets

$$\begin{aligned} O &= (0,0), O_{-1}^1 = \left(\frac{1 + k_1a}{k_1\left(2 + c_1\right)}, 0\right), \\ O_{-1}^2 &= \left(0, \frac{1 + k_2a}{k_2\left(2 + c_2\right)}\right), \\ O_{-1}^3 &= \left(\frac{a\left(2 + c_2 - d\right)k_1k_2 + \left(2 + c_2\right)k_2 - dk_1}{k_1k_2\left[\left(2 + c_1\right)\left(2 + c_2\right) - d^2\right]}, \frac{a\left(2 + c_1 - d\right)k_1k_2 + \left(2 + c_1\right)k_1 - dk_2}{k_1k_2\left[\left(2 + c_1\right)\left(2 + c_2\right) - d^2\right]}\right). \end{aligned} \tag{13}$$

This means that the origin point belongs to zone Z_4. For convenience, let $w_1 = OO_{-1}^1$ and $w_2 = OO_{-1}^2$ be two segments on the invariant axes q_1 and q_2. Let also w_1^{-1} and w_2^{-1} be their rank-1 preimages, respectively. So at any points $(u, 0) \in w_1$ and $(0, v) \in w_2$, their rank-1 preimages will satisfy the following algebraic systems:

$$\begin{cases} u = q_1(t) + k_1q_1(t)\left(a - \left(2 + c_1\right)q_1(t) - dq_2(t)\right), \\ 0 = q_2(t) + k_2q_2(t)\left(a - \left(2 + c_2\right)q_2(t) - dq_1(t)\right), \\ 0 = q_1(t) + k_1q_1(t)\left(a - \left(2 + c_1\right)q_1(t) - dq_2(t)\right), \\ v = q_2(t) + k_2q_2(t)\left(a - \left(2 + c_2\right)q_2(t) - dq_1(t)\right). \end{cases} \tag{14}$$

So both w_1^{-1} and w_2^{-1} can be presented by

$$\begin{aligned} w_1^{-1} &: q_2 = 0 \text{ or } 1 + k_2\left(a - \left(2 + c_2\right)q_2(t) - dq_1(t)\right) = 0, \\ w_2^{-1} &: q_1 = 0 \text{ or } 1 + k_1\left(a - \left(2 + c_1\right)q_1(t) - dq_2(t)\right) = 0. \end{aligned} \tag{15}$$

As one can see in Figure 2, those lines intersect at point O_{-1}^3.

4. Fixed Points and Stability

By setting $q_i(t + 1) = q_i(t) = \overline{q}$ in map (9), the following fixed points are obtained:

$$\begin{aligned} E_o &= (0,0), E_1 = \left(\frac{a}{2 + c_1}, 0\right), E_2 = \left(0, \frac{a}{2 + c_2}\right), \\ E_* &= \left(\frac{a\left(2 + c_2 - d\right)}{\left(2 + c_1\right)\left(2 + c_2\right) - d^2}, \frac{a\left(2 + c_1 - d\right)}{\left(2 + c_1\right)\left(2 + c_2\right) - d^2}\right). \end{aligned} \tag{16}$$

Since $a > 0, c_i > 0, i = 1, 2$ and $d \in [-1, 1]$, it is clear that all the fixed points are positive. The following propositions are raised, and their proofs are given in Appendix A.

Proposition 1. *The boundary equilibrium point $E_o = (0, 0)$ is an unstable repelling node.*

Proposition 2. *The boundary equilibrium point $E_1 = ((a/2 + c_1), 0)$ is a saddle point if $0 < k_1 < (2/a)$. Otherwise, it is an unstable node.*

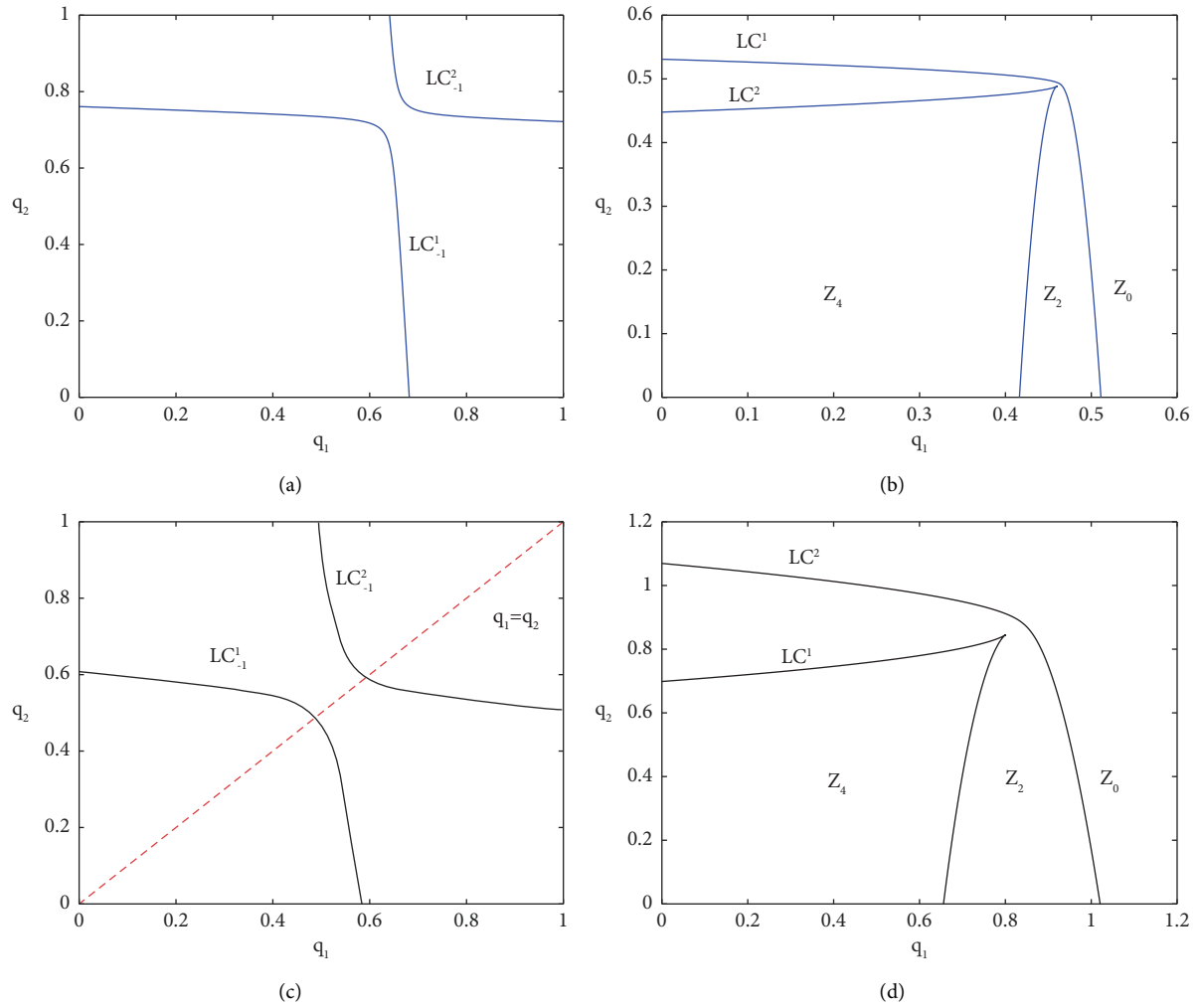

FIGURE 1: The critical curves of map (9). (a) The preimages of critical curve LC represented by (11) at the parameters values, $a = 1, c_1 = 0.2, c_2 = 0.3, k_1 = 0.5, k_2 = 0.4$, and $d = 0.2$. (b) The critical curves $\mathrm{LC} = T(\mathrm{LC}_{-1})$ at the same parameters as of (a). (c) The preimages of critical curve LC represented by (11) at the parameters values, $a = 2, c_1 = 0.4, c_2 = 0.3, k_1 = 1.25, k_2 = 1.26$, and $d = 0.5$. (d) The critical curves $\mathrm{LC} = T(\mathrm{LC}_{-1})$ at the same parameters as of (c).

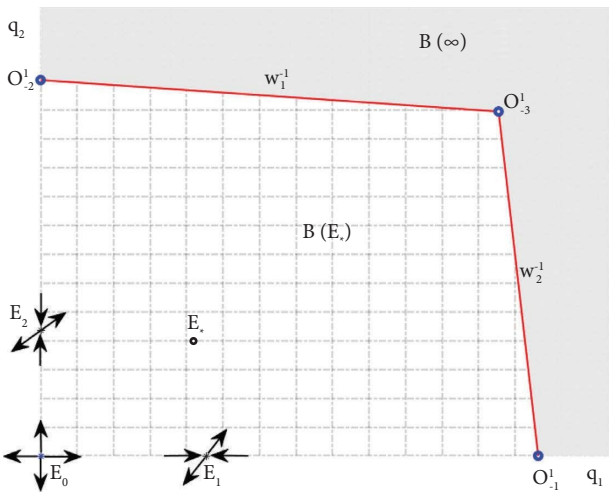

FIGURE 2: The basin of attraction of Nash equilibrium point E_* at the parameters values, $a = 1, c_1 = 0.2, c_2 = 0.3, k_1 = 0.5, k_2 = 0.5$, and $d = 0.2$.

Proposition 3. *The boundary equilibrium point* $E_2 = (0, (a/2 + c_2))$ *is a saddle point if* $0 < k_2 < (2/a)$. *Otherwise, it is an unstable node.*

Proposition 4. *The point* E_* *is called the Nash equilibrium point and is asymptotically stable if*

$$k_1 k_2 > \frac{(2 + c_1)}{a(2 + c_1 - d)} k_1 + \frac{(2 + c_2)}{a(2 + c_2 - d)} k_2. \tag{17}$$

Proposition 5. *The Nash point loses its stability due to flip bifurcation if*

$$k_1 k_2 < \frac{(2 + c_1)}{a(2 + c_1 - d)} k_1 + \frac{(2 + c_2)}{a(2 + c_2 - d)} k_2. \tag{18}$$

Figure 2 presents the basin of attraction of Nash point which looks like a regular convex polygon whose vertices are

the four preimages of the origin. It can be seen that both w_1^{-1} and w_2^{-1} divide the phase plane into two parts $B(E_*)$ and $B(\infty)$. The first part $B(E_*)$ contains all points which generate bounded trajectories converging to the Nash point, i.e., $B(E_*) = \{(q_1, q_2) \in \mathbb{R}_+^2 : T^t(q_1, q_2) \longrightarrow E_*, t \longrightarrow \infty\}$, while the second part $B(\infty)$ consists of all points which generate unbounded trajectories colored by gray. It can also be seen that the boundaries of $B(E_*)$ and $B(\infty)$ are equal, i.e., $\partial B(E_*) = \partial B(\infty)$.

4.1. Local Bifurcation. Map (9) presents a dynamical system that contains two important parameters k_1 and k_2. These parameters are called the speed of adjustment parameters and any slight change in them may raise a great change in the dynamics of the system. These parameters are selected to be the bifurcation parameters. Let us assume the following values, $a = 1, c_1 = 0.2, c_2 = 0.3, d = 0.2$, and $k_1 = 0.5$ (or $k_2 = 0.5$) on varying k_2 (or on varying k_1). Figures 3(a) and 3(b) show the influence of the speed parameters on the stability of the Nash point. Both parameters undergo a flip bifurcation diagram. Fixing those parameters and changing the value of d present its impact on the stability region of Nash point. Numerical experiments show that increasing d close to 1 makes the region of stability with respect to the speed parameters increase. On the other hand, at the values, $a = 2, c_1 = 0.4, c_2 = 0.3, d = 0.5$, and $k_1 = 1.25$ (or $k_2 = 1.26$) on varying k_2 (or on varying k_1), Figures 3(c) and 3(d) show that the period-4 cycle emanating from the flip bifurcation may undergo a Neimark–Sacker one as both the speed parameters increase. Keeping the value of speed parameters relatively small keeps system (9) in a stable state. Furthermore, as d increases to be close to 1, the region of stability with respect to the speed parameters is also extended. Conversely, as the parameter a increases while the other parameter values are fixed, the stability region is decreased with respect to the speed parameters. To end this local analysis, we plot in Figure 4 the influence of the parameter a on the map's dynamics at the values, $c_1 = 0.4, c_2 = 0.3, d = 0.95, k_1 = 1.25$ and $k_2 = 1.26$.

5. The Invariant Manifold

The point (0, 0) for map (9) has an important aspect. If the map initiates from this point it will be directly trapped to this point. This means that if $q_1(t) = 0$ or $q_2(t) = 0$, then $q_1(t+1) = 0$ or $q_2(t+1) = 0$ and hence the coordinates axes $\overrightarrow{Oq_1}$ and $\overrightarrow{Oq_2}$ become invariant. Those axes construct an invariant manifold for T, and then, its dynamics can be described by a one-dimensional map as follows:

$$q_i(t+1) = (1 + k_i a)\left[1 - \frac{k_i(2 + c_i)}{1 + k_i a} q_i(t)\right] q_i(t), \quad i = 1, 2. \tag{19}$$

We see that map (19) is topologically equivalent to

$$y_i(t+1) = \mu_i y_i(t)(1 - y_i(t)), \quad i = 1, 2, \tag{20}$$

through the linear transformation given as

$$q_i = \frac{1 + k_i a}{k_i(2 + c_i)} y_i, \quad i = 1, 2, \tag{21}$$

and $\mu_i = 1 + k_i a, i = 1, 2$.

5.1. Dynamic Analysis. For map (20), let us consider the following function:

$$\sigma(y) = \mu y(1 - y). \tag{22}$$

This function presents the well-known logistic equation with a parameter μ causing its dynamics. The first derivative, $\sigma'(y) = \mu(1 - 2y)$ attains a function maximum value occurring at $\mu/4$ and the point $y = 1/2$. It is clear that $\sigma(0) = 0$ and $\sigma(1) = 0$, which means that $\sigma(y) \in [0, 1)$ and $0 < \mu < 4$ for all $y \in [0, 1]$. It is also simple to see that map (20) has two fixed points, $\overline{y} = 0$ and $\overline{y} = 1 - (1/\mu)$, which are nonnegative provided that $\mu > 1$. One can see that $\sigma'(0) = \mu$ and then the fixed point $\overline{y} = 0$ is stable if $\mu \in (0, 1)$, otherwise it is unstable. The point, $\overline{y} = 1 - (1/\mu)$, is stable if $\mu \in (1, 3)$, otherwise it is unstable if $\mu > 3$. Figure 5(a) demonstrates the bifurcation diagram of map (20) on varying parameter μ. As mentioned above, its dynamics is similar to the well-known standard logistic map. Figures 5(b) and 5(c) illustrate the cobweb diagrams of map (20) at different values of the parameter μ. When $0 < \mu < 1$, the fixed point $\overline{y} = 0$ becomes stable but when $\mu = 1$, a transcritical bifurcation emerges. At $1 < \mu < 3$, the fixed point $\overline{y} = 1 - (1/\mu)$ gets stable resulting in a stable period-2 cycle at $\mu = 3$ as shown in Figure 5(b). At $\mu = 3.9$, the period-2 cycle becomes unstable around the fixed point as shown in Figure 5(c) on which a chaotic trajectory is born.

Proposition 6. *At the critical value, $k_i = (2/a), i = 1, 2$, the trajectories of T beginning on the invariant axes $\overrightarrow{Oq_1}$ and $\overrightarrow{Oq_2}$ diverge when $k_i \in ((2/a), +\infty), i = 1, 2$.*

Proof. The proof is straightforward. Using $\mu_i = 1 + k_i a, i = 1, 2$ and $\mu_i > 3, i = 1, 2$, we complete the proof. □

5.2. The Symmetric Case. Map (9) possesses an important aspect. At the assumption $k_i = k, c_i = c; i = 1, 2$, the map becomes symmetric. It means that if q_1 and q_2 are swapped, the structure of the map does not change, i.e., $T \circ \mathrm{F} = \mathrm{F} \circ \mathrm{T}$, where $F : (q_1, q_2) \longrightarrow (q_2, q_1)$. Consequently, the diagonal set defined by $\Delta = \{(q_1, q_2) : q_1 = q_2\}$ constructs an invariant manifold. This implies that the dynamics of any trajectories which start on the diagonal set $(q_1(0) = q_2(0))$ will come back to the diagonal set at each time step t. So the dynamics of map (9) can be studied by a one-dimensional map under the restriction given on Δ as follows:

$$T_\Delta : \dot{q} = h(q) := q + kq[a - (2 + c + d)q]. \tag{23}$$

Now, for any synchronized trajectories (i.e., $q_1(t) = q_2(t)$ at every time period t), they will be governed by $T_\Delta : \Delta \longrightarrow \Delta$ and one gets the following proposition.

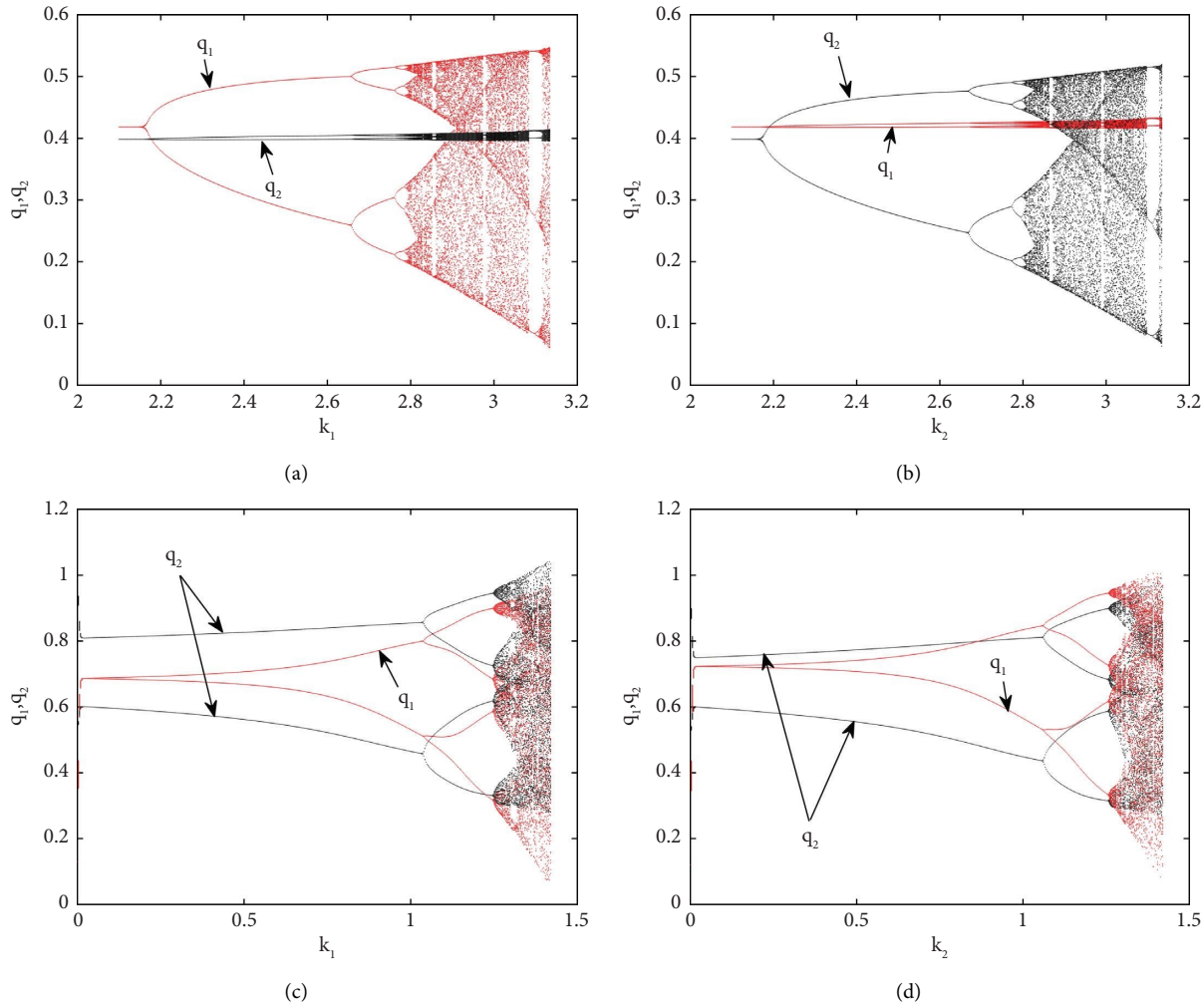

FIGURE 3: The bifurcation diagrams at the values, $a = 1, c_1 = 0.2, c_2 = 0.3, d = 0.2$, and (a) on varying k_1 with $k_2 = 0.5$. (b) On varying k_2 with $k_1 = 0.5$. The bifurcation diagrams at the values, $a = 2, c_1 = 0.4, c_2 = 0.3, d = 0.5$, and (c) on varying k_1 with $k_2 = 1.25$. (d) On varying k_2 with $k_1 = 1.26$.

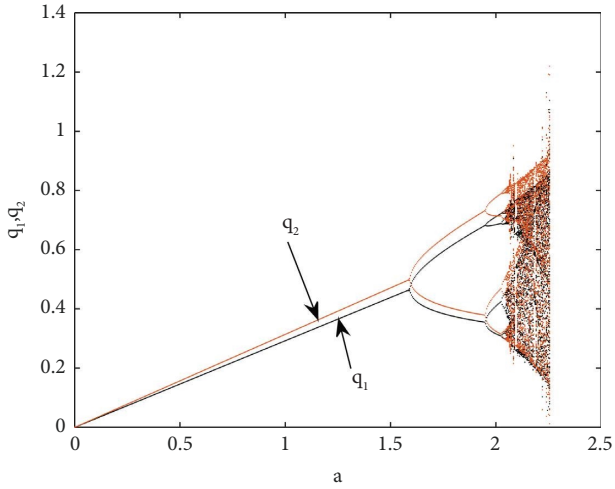

FIGURE 4: The influence of the parameter a on the dynamics of map (9) at the values, $c_1 = 0.4, c_2 = 0.3, d = 0.95, k_1 = 1.25$, and $k_2 = 1.26$.

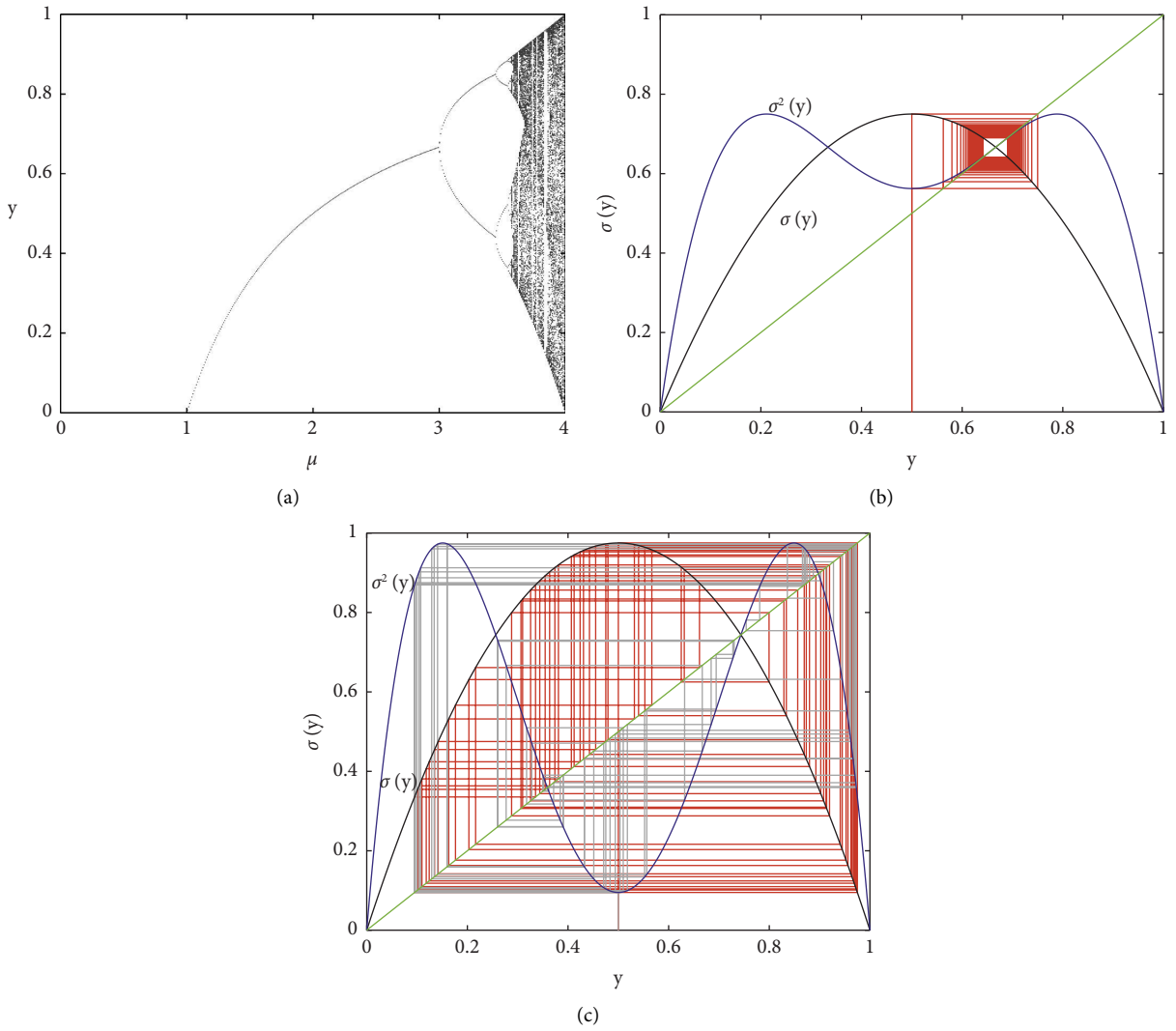

FIGURE 5: (a) The 1D bifurcation diagram of map (20) with respect to μ. (b) The cobweb diagram for a stable fixed point at $\mu = 3$ where $\sigma^2(y)$ is the second iteration of $\sigma(y)$. (c) The cobweb for a chaotic situation occurring at $\mu = 3.9$.

Proposition 7. *Map (23) is characterized as unimodal and concave and* $\lim_{q\longrightarrow 0^+} h(q) = 0$ *and* $\lim_{q\longrightarrow +\infty} h(q) = -\infty$. *It means that it possesses a threshold point* $\overline{q} = (a/2 + c + d)$ *that occurs at* $h(\overline{q}) = 0$. *The unimodal aspect means that there is a critical point given by*

$$q_{cr} = \frac{1 + ka}{2k(2 + c + d)}. \tag{24}$$

Proof. It is easy to see that the second derivative of $h(q)$ is nonpositive for all q and hence $h(q)$ has only one global maximum value at q_{cr} without any local maximum. This means that the function $h(q)$ is unimodal and concave with $\acute{h}(q_{cr}) = 0$. □

Now, the map T_Δ possesses only one nonzero fixed point that is $\overline{q}$ which is locally stable if $k < (2/a)$, while flip bifurcation occurs at $k = k_f := (2/a)$. Figure 6 shows the

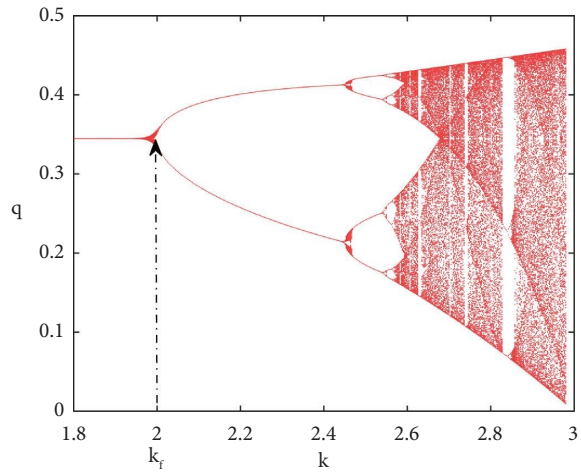

FIGURE 6: The 1D bifurcation of the map T_Δ on varying the parameter k at the values, $a = 1, c = 0.4$, and $d = 0.5$.

one-dimensional bifurcation diagram where flip bifurcation occurs at $k_f = 2$.

6. Basin of Attraction

Let us now investigate additional properties for map (19) such as its basin. The map can be rewritten in the following form:

$$\acute{q}_i = g_i(q_i) \coloneqq q_i[1 + k_i a - k_i(2 + c_i)q_i], \quad i = 1, 2. \tag{25}$$

Following [43], the invariant axes and their preimages of any rank can be used to form the boundaries of nondiverging trajectories. Map (25) possesses a positive fixed point $q_i^* = (k_i a/k_i(2 + c_i)), i = 1, 2$. One can easily see that $g_i(q_i)$ is a concave function and an increasing function if $q_i < (1 + k_i a/2k_i(2 + c_i))$. In addition, for any point $(q_1, 0), q_1 > 0$ or $(0, q_2), q_2 > 0$, it gives $\acute{q}_1 > 0, \acute{q}_2 = 0$ or $\acute{q}_1 = 0, \acute{q}_2 > 0$. In contrast, if $q_i > (1 + k_i a/2k_i(2 + c_i))$, then $g_i(q_i)$ is concave and unimodal. In the latter case, one can get the nonnegative points $\widetilde{q}_i^{bo} = (1 + k_i a/k_i(2 + c_i))$ and $\widetilde{q}_i^{cr} = (1 + k_i a/2k_i(2 + c_i))$ at $\acute{q}_i = 0$ and $\acute{g}_i(\widetilde{q}_i^{cr}) = 0$, respectively. If $g_i(\widetilde{q}_i^{cr}) < \widetilde{q}_i^{bo}$, i.e., if $k_i a < 3$, then it means that the bounded trajectories along the invariant axes $\overrightarrow{Oq_1}$ and $\overrightarrow{Oq_2}$ are bounded provided that the initial states lie on the segment $w_i = [O, O_i^{-1}], i = 1, 2$, where $O_i^{-1} = \widetilde{q}_i^{bo} \neq 0$ presents rank-1 preimages for the origin point. Conversely, any other trajectories starting on those axes for initials outside ω_i become infeasible (or nondiverging) trajectories. Moreover, the eigenvalues at a point (q_1, q_2) on those invariant axes become $\widetilde{\lambda}_i = 1 + ak_i - 2k_i(2 + c_i)q_i, i = 1, 2$. For example, at a point $(q_1, 0)$, one gets $\widetilde{\lambda}_1 = 1 + ak_1 - 2k_1(2 + c_1)q_1$ and $\widetilde{\lambda}_2 = 1 + ak_2$, which means that trajectories with positive initial states beginning close to those axes are repelled by them. Figure 7 presents the basin of attraction of the point (q_1^*, q_2^*) and period-4 cycle marked by the colors brown and blues, respectively. This cycle is born at the values $a = 2, c_1 = 0.4, c_2 = 0.3, k_1 = 1.25$, and $k_2 = 1.26$. The other colors that are gray and white are for the divergence and nonconvergence points. It is easy to see that the lines $w_i, i = 1, 2$ and their inverses $w_i^{-1}, i = 1, 2$ separate the divergence and nonconvergence points.

6.1. Global Analysis. In economic models, it is necessary to globally investigate the topological structure of the basin of attraction. This structure does not appear when carrying out local analysis. Analyzing the behavior of map (9) in the long-run whose variables take intials values not close to the equilibrium point is necessary in order to see the qualitative changes that may be occurred in the topological structure. Numerically, two cases for map (9) that are the asymmetric and symmetric cases are investigated in this subsection. First, the asymmetric case is studied at two different sets of parameter values as follows. We start with the first set, $(a, c_1, c_2, d) = (1, 0.2, 0.3, 0.5)$. Figure 8(a) shows the two-

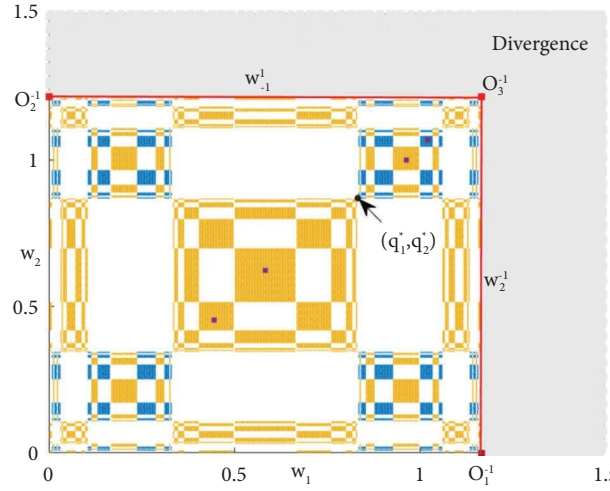

FIGURE 7: The basin of attraction for the period-4 cycle at the values, $a = 2, c_1 = 0.4, c_2 = 0.3, k_1 = 1.25$, and $k_2 = 1.26$.

dimensional bifurcation diagram in the (k_1, k_2) – *plane*. The gray color illustrates the stability region of the equilibrium point E_* while the other colors present different types of period cycles marked by $2, 4,$ and $6, \ldots$. Assuming $k_1 = 2.0801556$ and $k_2 = 3.02933$, Figure 8(b) shows the basin of period-7 cycle marked by squares. Its basin is colored in light blue while the yellow color is for the basin of the equilibrium point E_*. It can be seen from the figure that the infeasible region colored in gray is disconnected. It is clear that some holes of this region lie within the basin of cycle 7. This is because of the contact bifurcation that took place. This contact bifurcation is discussed in Figure 8(c) in detail. Figure 8(c) presents the basin of attraction of a chaotic attractor (marked by green) that occurred at the values, $(a, c_1, c_2, d, k_1, k_2) = (1, 0.2, 0.3, 0.5, 3.04278, 2.072089)$. This chaotic attractor is distributed in the zones, Z_4 and Z_2. As one can see, the infeasible region (or the escaping domain) is disconnected. It is clear that the whole region does not lie in Z_0 and part of it denoted by h_o enters the region Z_2. The part h_o is constructed due to the intersection between the critical curve branch LC^1 and the boundary line w_2^{-1}. It consists of two parts connected by the branch LC_{-1}^2. This part belongs to the zone Z_2 whose points possess two distinct real rank-1 preimages and are responsible for the disconnection of the escaping domain and the coexistence of main hole h_{-1} that entirely lies in Z_4. The main hole h_{-1} is formed by two parts $h_{-1}^{(1)}$ and $h_{-1}^{(2)}$ connected by the branch LC_{-1}^1. Each point belonging to the main hole will have four distinct real rank-2 preimages. Numerical simulation shows that points in the main hole are responsible for constructing the small holes denoted by $h_{-2}^{(1)}, h_{-2}^{(2)}, h_{-2}^{(3)}$, and $h_{-2}^{(4)}$. So it is obvious from the Figures 8(b) and 8(c) that contact bifurcation has occurred and consequently holes from the infeasible domain are born. It is also seen that the structure of the basins for the period-7 cycle and chaotic attractor is bounded by the quadrilateral shape $OO_1^{-1}O_3^{-1}O_2^{-1}$. Such complicated structures make the future evolution of the game unpredictable in case players take initial states inside those holes.

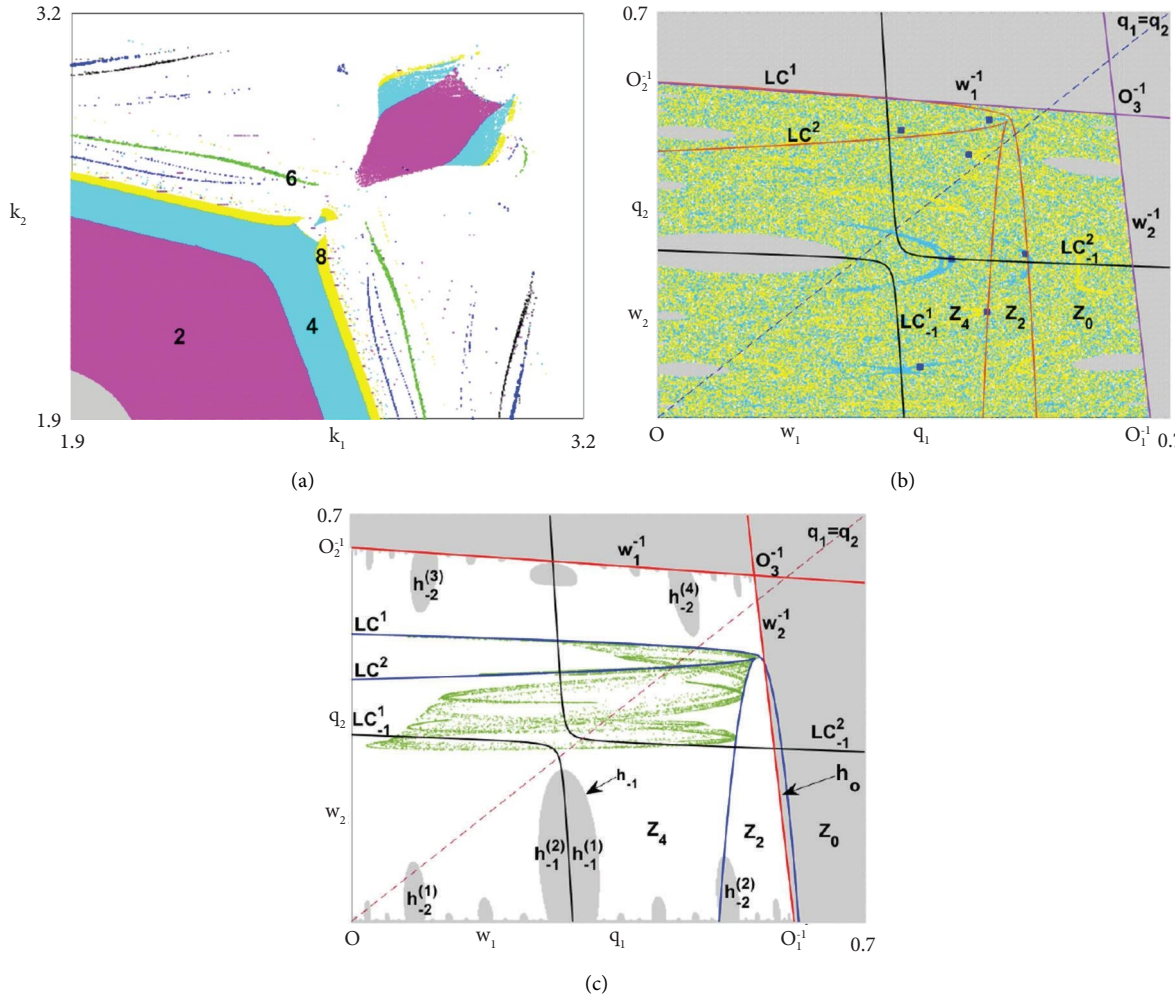

FIGURE 8: (a) The two-dimensional bifurcation diagram at the first set of values, $(a, c_1, c_2, d) = (1, 0.2, 0.3, 0.5)$. The gray color represents the stability region for E_* while the other colors are for different period cycles as given in the graph. (b) The basin of attraction of the period-7 cycle at the values $(a, c_1, c_2, d, k_1, k_2) = (1, 0.2, 0.3, 0.5, 2.0801556, 3.02933)$. (c) The basin of attraction of chaotic attractor at the values $(a, c_1, c_2, d, k_1, k_2) = (1, 0.2, 0.3, 0.5, 3.04278, 2.072089)$.

Then, we investigate the dynamics of map (9) using another set of values. Let us assume the values, $(a, c_1, c_2, d, k_1, k_2) = (2, 0.4, 0.3, 0.5, 1.27, 1.26)$. At this set, the dynamics of map (9) are represented by four closed rings around the equilibrium point due to Neimark–Sacker taking place after the period-4 cycle. Keeping the set of values fixed but by increasing k_1 to 1.29, the four rings turn into a four-band chaotic attractor. The basin of attraction of this chaotic attractor with the equilibrium point is plotted in Figure 9(b). As one can see that the origin point belongs to Z_4 and the chaotic attractor is distributed in zones Z_4 and Z_2. By further increasing the speed parameter k_1 to 1.3, the chaotic attractor is converted into period-16 cycle. This cycle has a basin of attraction bounded by the quadrilateral shape $OO_1^{-1}O_3^{-1}O_2^{-1}$. This period cycle is turned into a four-band chaotic attractor as k_1 increases to 1.32 as shown in Figure 9(d). Keeping the other values fixed and by increasing the speed parameter to the value $k_1 = 1.4$ a two-band chaotic attractor emerges whose basin is given in Figure 9(e). As one can see that as the speed parameter increases the critical branch LC^1 is approaching to the boundary w_2^{-1}. When the speed parameter reaches the value 1.449, one gets a one-band chaotic attractor whose attractive basin is given in Figure 9(f) and then LC^1 becomes tangent to the boundary w_2^{-1}. This tangentiality causes the contact bifurcation and makes the infeasible domain disconnected due to the holes coexisting in the attracting domain.

In contrast, let us now investigate the symmetric case of map (9). This case occurred by assuming that $k_1 = k_2 = k, c_1 = c_2 = c$ and hence map (9) can be rewritten as follows:

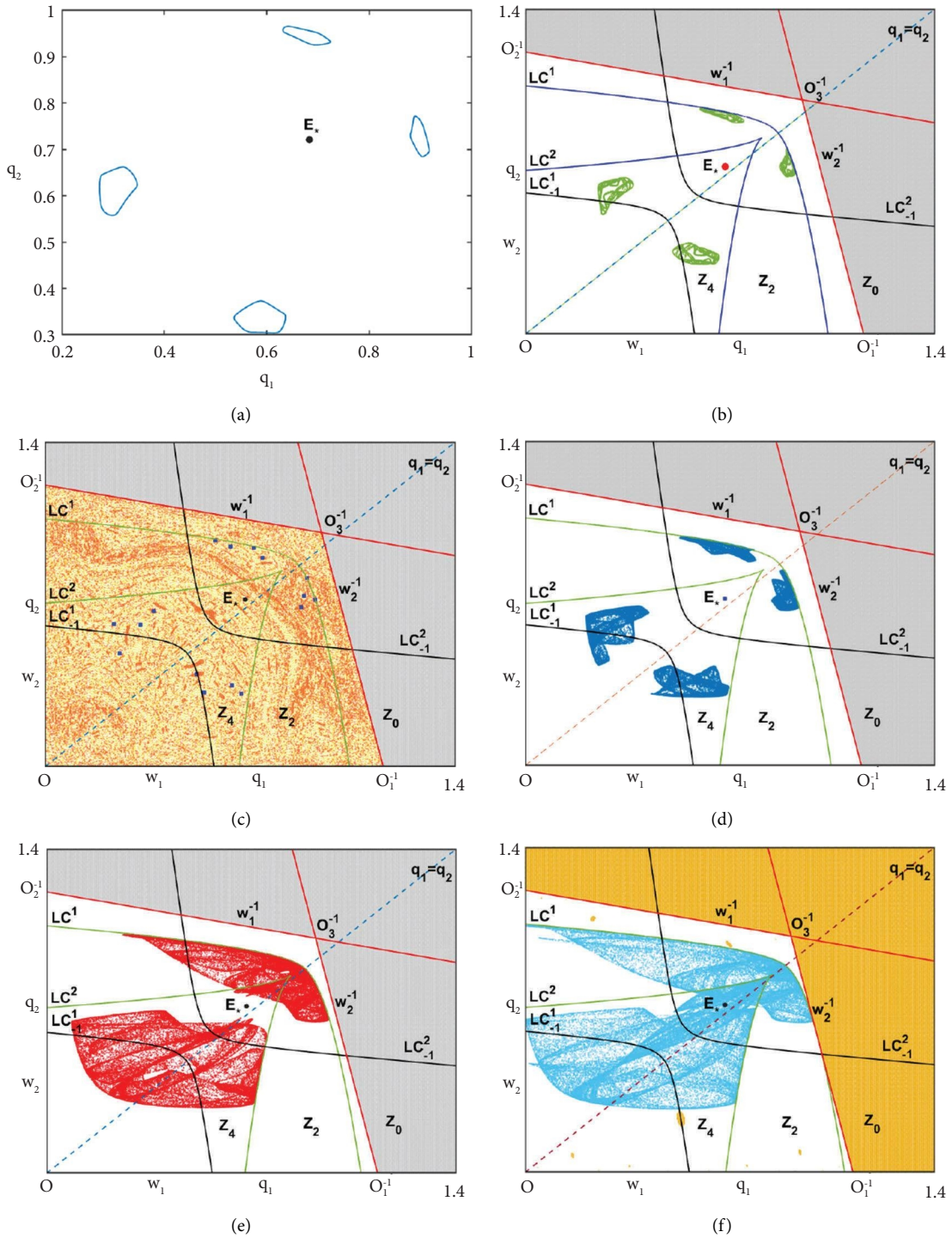

FIGURE 9: At $(a, c_1, c_2, d, k_2) = (2, 0.4, 0.3, 0.5, 1.26)$: (a) The phase plane for four rings at $k_1 = 1.27$. (b) The phase plane and basin of attraction for the chaotic attractor at $k_1 = 1.29$. (c) The basin of attraction of period-16 cycle at $k_1 = 1.30$. The phase plane and basin of attraction for the chaotic attractor (d) at $k_1 = 1.32$. (e) $k_1 = 1.4$. (f) $k_1 = 1.449$.

$$T_s(q_1, q_2): \begin{cases} q_1(t+1) = q_1(t) + kq_1(t)(a - (2+c)q_1(t) - dq_2(t)), \\ q_2(t+1) = q_2(t) + kq_2(t)(a - (2+c)q_2(t) - dq_1(t)). \end{cases} \tag{26}$$

It is easy to see that map (26) is symmetric on the diagonal $\Delta := \{(q_1, q_2) \in \mathbb{R}^2_+ : q_1 = q_2\}$. In this case, there is no mathematical meaning for the equilibrium points except the point $E_s = ((a/2 + c + d), (a/2 + c + d))$ which belongs to the diagonal Δ. The local stability of this point around Δ is related to synchronization (intermittency). Simply, one can

say that a synchronous dynamic behavior is obtained if there exists a period of time $\hat{t}$ such that $q_1(t) = q_2(t)$ for any $t > \hat{t}$. So, the Jacobian of map (26) is given by

$$J(q_1, q_2) = \begin{pmatrix} \ell(q) & m(q) \\ m(q) & \ell(q) \end{pmatrix},$$
$$\ell(q) = 1 + k[a - (4 + 2c + d)q], \tag{27}$$
$$m(q) = -kdq,$$

where the eigenvalues are represented as

$$\lambda_{\parallel} = \ell(q) + m(q) = 1 + k[a - 2(2 + c + d)q],$$
$$\lambda_{\perp} = \ell(q) - m(q) = 1 + k[a - 2(2 + c)q], \tag{28}$$

and the corresponding eigenvectors are (1, 1) and $(1, -1)$, respectively. Thus, the following proposition is obtained.

Proposition 8. *The local stability of the equilibrium point E_s is achieved if $k < (2/a)$. A flip bifurcation is raised if $k = k_f = (2/a)$.*

Proof. Substituting E_s in (28), one gets the following eigenvalues:

$$\lambda_{\parallel} = 1 - ka\left(\frac{2 + c - d}{2 + c + d}\right),$$
$$\lambda_{\perp} = 1 - ka. \tag{29}$$

Here, $|\lambda_{\perp}| < 1$ and $|\lambda_{\parallel}| < 1$ give $k < (2/a)$ and $k < (2/a)(2 + c + d/2 + c - d)$, respectively. Thus, combining the two conditions completes the proof. □

The following figures simulate the abovementioned proposition. Let us assume $a = 2, c = 0.4, k = 1.4$ and $d = 0.5$. Figure 10(a) shows that at $k = k_f = 1$, the period-2 cycle and hence the one-dimensional flip bifurcation is obtained on varying the speed parameter k. Figure 10(b) presents the time series for both decision variables. One can observe from Figure 10(c) (which represents the displacement $q_1 - q_2$ with time t) that the transient behaviors of map (25) may be described by bursts that appear outside the diagonal Δ. Therefore, intermittency will occur in map (25) as shown in Figure 10(d). Figure 10(e) shows a complex chaotic attractor raised entirely on the diagonal Δ at the parameters values, $(a, c, k, d) = (2, 0.4, 1.4, 0.5)$ with bursts out of the diagonal Δ. With a slight increase in the speed parameter k with 2×10^{-3} at the same parameter values, the weak attractor given in Figure 10(d) turns into a complex chaotic attractor depicted in Figure 10(e). As one can see, the equilibrium point E_s lies on the diagonal Δ and the chaotic attractor is not symmetric around the diagonal due to bursts raised on both sides as shown in Figure 10(f).

From the abovementioned proposition and analysis, it is clear that the speed parameter k affects the stabilization of the equilibrium point E_s. It is noted that the high reactivity of the competing firms to the marginal profit should coexist. Moreover, suppose a k–cycle given by $\{(q_1, q_1), \ldots, (q_m, q_m)\}$ of the map T_s embedded into the invariant diagonal Δ corresponding to the cycle $\{q_1, \ldots, q_m\}$. Therefore, this $k-$ cycle has multipliers given by

$$\lambda_{\parallel}^{k} = \prod_{i=1}^{k} (\ell(q_i) + m(q_i)),$$
$$\lambda_{\perp}^{k} = \prod_{i=1}^{k} (\ell(q_i) - m(q_i)), \tag{30}$$

with corresponding eigenvectors (1, 1) and $(1, -1)$. So, the stability of E_s is guaranteed by $|\lambda_{\perp}| < 1$ and is confirmed by $|\lambda_{\parallel}| < 1$. For a complex chaotic attractor H of the map (25), H is asymptotically stable if and only if all trajectories of H are transversely attracting. This asymptotic stability condition of H is obtained based on the transverse Lyapunov exponent as follows:

$$\Lambda_{\perp} = \lim_{n \longrightarrow \infty} \sum_{i=1}^{n} \ln |\lambda_{\perp}(q(i))|, \tag{31}$$

where $q(0) \in H$ and $q(i)$ are the trajectories constructed by the map, and

$$T_s : q(t + 1) = q(t) + kq(t)[a - (2 + c + d)q(t)]. \tag{32}$$

The definitions are given ([42, 43]) as follows.

Definition 9. An asymptotically stable chaotic attractor H is Lyapunov stable if for every neighborhood U of H there exists a neighborhood V of H such that $T^n(V) \subset U \; \forall n \geq 0$ and its basin $B(H)$ has a neighborhood of H.

Definition 10. A spectrum of Lyapunov exponent is defined based on the initial conditions as follows:

$$\Lambda_{\perp}^{\min} < \ldots < \Lambda_{\perp}^{nat} < \ldots < \Lambda_{\perp}^{\max}, \tag{33}$$

where $\Lambda_{\perp}^{nat}$ denotes a Lyapunov exponent obtained at a generic trajectory in H. *If* $\Lambda_{\perp}^{\max} < 0$, then a set is called a Lyapunov attractor. When $\Lambda_{\perp}^{\max} > 0$ and $\Lambda_{\perp}^{nat} < 0$, then a set is no longer Lyapunov stable and gets a Milnor attractor. Milnor attractor is defined as follows.

Definition 11. A closed invariant set H is called a weak attractor in Milnor sense if its stable set (the basin of attraction) $B(H)$ has a positive Lebesgue measure.

6.2. Independent Firms. In this subsection, we study a particular case in which competing firms behave as if they were monopolistic firms with independent products, that is $d = 0$. In this case, map (25) can be rewritten as follows:

$$T_s(d = 0) : \begin{cases} q_1(t + 1) = q_1(t) + kq_1(t)(a - (2 + c)q_1(t)), \\ q_2(t + 1) = q_2(t) + kq_2(t)(a - (2 + c)q_2(t)), \end{cases} \tag{34}$$

which represents a diagonal map. It is easy to see that the abovementioned map conjugates the logistic map, $x(t + 1) = \mu x(t)(1 - x(t))$ with $\mu = 1 + ka$. The eigenvalues of the abovementioned map $\lambda_{\perp} = 1 - ka - 2k(2 + c)q_1$ and

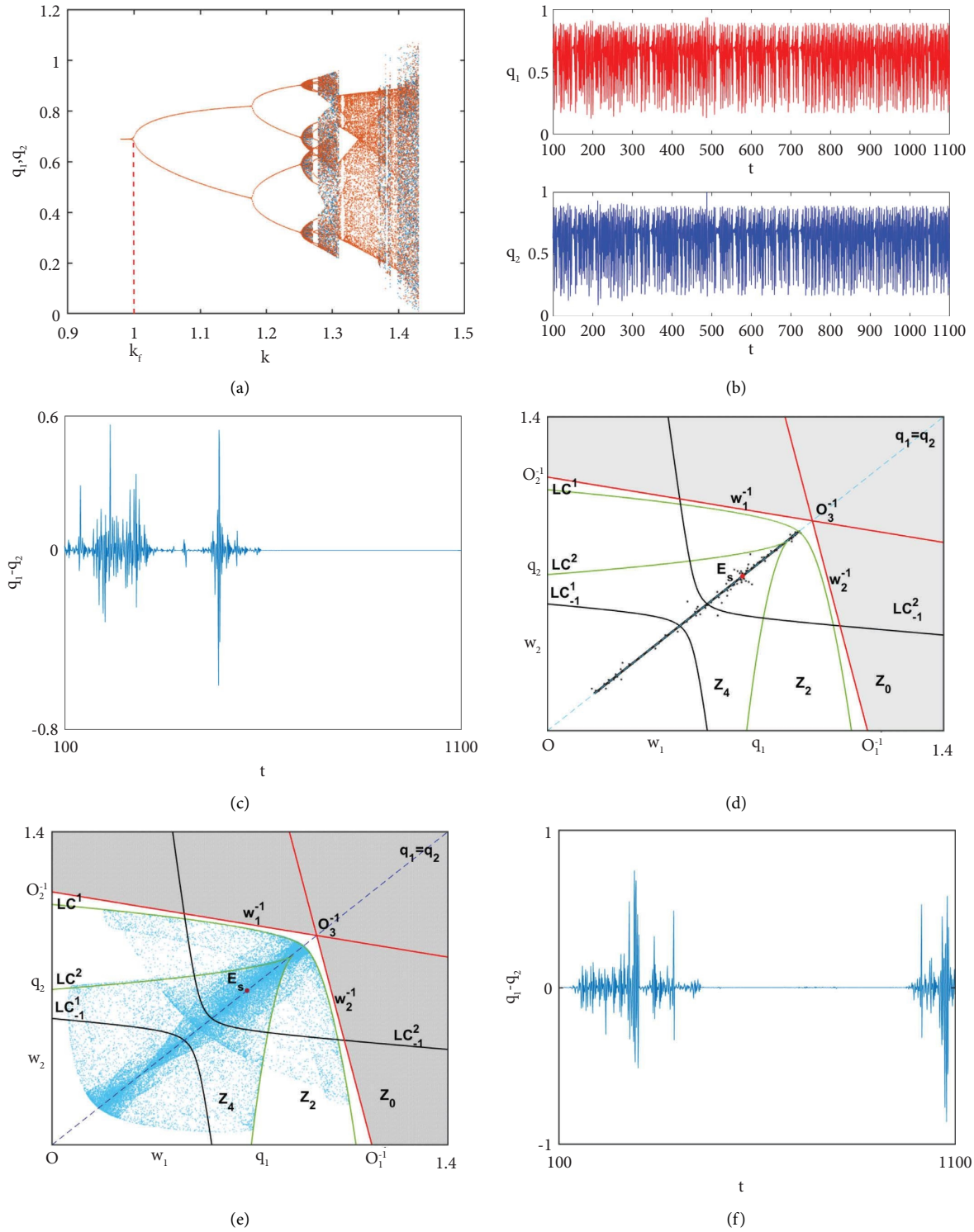

Figure 10: (a) The 1D bifurcation diagram on varying the speed parameter k at the values, $a = 2, c = 0.4$, and $d = 0.5$. (b) The time series for q_1 and q_2 at the values, $(a, c, k, d) = (2, 0.4, 1.4, 0.5)$. (c) Bursts away from Δ before synchronization takes place at the initial state $(q_1(0), q_2(0)) = (0.13, .012)$ and $(a, c, k, d) = (2, 0.4, 1.4, 0.5)$. (d) Complex weak chaotic attractor raised at the values, $(a, c, k, d) = (2, 0.4, 1.4, 0.5)$. (e) Complex chaotic attractor raised at the values, $(a, c, k, d) = (2, 0.4, 1.402, 0.5)$. (f) The time series for $q_1 - q_2$ at the values, $(a, c, k, d) = (2, 0.4, 1.402, 0.5)$.

$\lambda_{\parallel} = 1 - ka - 2k(2 + c)q_2$ are symmetric. This means that any attracting set along the diagonal will have identical eigenvalues. Due to this property, any period-doubling bifurcation that has taken place along the diagonal (which is also associated with the cascade bifurcation with the well-known logistic map) will be followed by a simultaneous

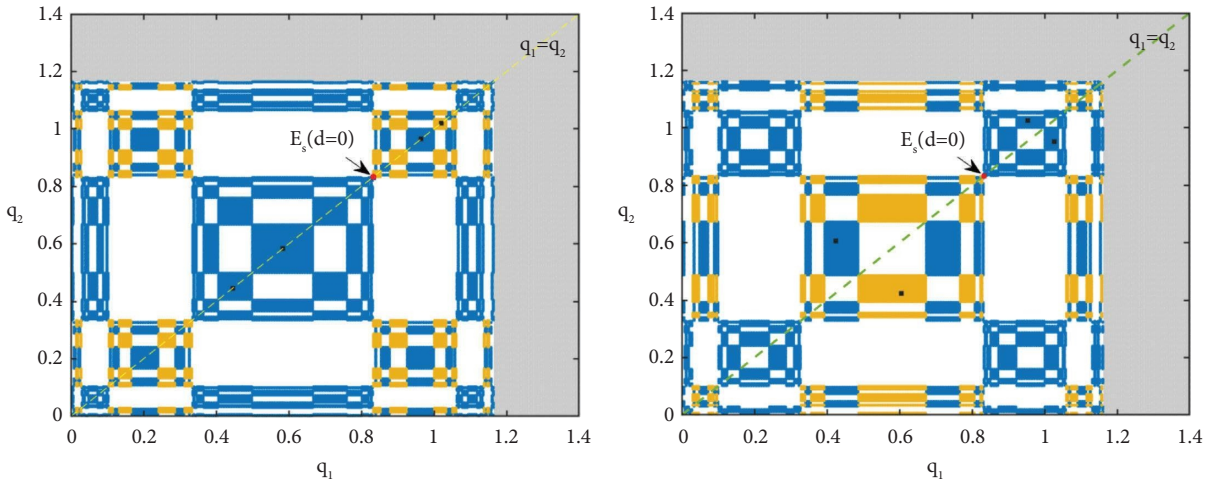

FIGURE 11: The basin of attraction of two different period-4 cycles at the parameter values, (a) $a = 2, c = 0.4$, and $k = 1.25$ and (b) $a = 2, c = 0.4$, and $k = 1.27$.

period-doubling bifurcation that has occurred along the symmetric direction. Hence the following proposition is raised.

Proposition 12. *The equilibrium point* $E_s(d = 0) = ((a/2 + c), (a/2 + c))$ *is locally stable if* $k < (2/a)$. *It loses its stability through period-doubling bifurcation at* $k = k_f = (2/a)$.

Proof. Substituting $E_s(d = 0) = ((a/2 + c), (a/2 + c))$ in (29) gives $|\lambda_\perp| < 1$ and $|\lambda_\parallel| < 1$ and this completes the proof.

At $a = 2$, one gets $k = k_f = 1$ and hence period-2 cycle is born. A further increase in k gives rise to high periodic cycles and hence flip bifurcation is obtained. Figure 11 shows the basin of attraction of two different period-4 cycles. The first one occurs at the values, $a = 2, c = 0.4$, and $k = 1.25$ and lies entirely on the diagonal. As k increases to 1.27, the second one is born but on both sides from the diagonal. This is due to the phenomena of multistability. □

7. Conclusion

Through this paper, the synchronization and multistability phenomena for a simple Cournot duopoly game whose cost has been computed based on the Cobb–Douglas utility function have been investigated. As in many relevant papers in the literature, the fixed points of the proposed game are obtained for the asymmetric case and their conditions of stability are investigated. Our obtained results have confirmed that the Nash equilibrium point may be unstable through flip bifurcation and under certain parameter values, Neimark–Sacker bifurcation has been born after the period-4 cycle. Some complex structures of basins for the nonlinear two-dimensional map describing the game have been discussed. Our discussion has shown that the game's map is noninvertible and its plane has been divided into three zones of preimages that are Z_0, Z_2, and Z_4. Furthermore, under certain parameter values the dynamics of the game's map behave as a weak chaotic attractor in Milnor's sense. This weak attractor has been distributed on the diagonal at which the synchronized trajectories arise. Any slight increase in the speed parameter has affected this weak attractor and converted it into a complicated one. Finally, the case when competing firms behave as if they were monopolistic firms with independent products has been studied showing the coexistence of two different period-4 cycles due to multistability.

The obtained results in this manuscript and their potential applications may be extended in future works for biological models and economic games with three competitors under different types of adjustment mechanisms. Furthermore, it may be also applied to economic games whose main interests are to optimize their objectives which include profits and social welfare.

Appendix

Map (9) admits the following Jacobian matrix:

$$J(q_1, q_2) = \begin{pmatrix} 1 + k_1[a - dq_2 - 2(2 + c_1)q_1] & -k_1 dq_1 \\ -k_2 dq_2 & 1 + k_2[a - dq_1 - 2(2 + c_2)q_2] \end{pmatrix}. \tag{A.1}$$

Proof of Proposition 1. At E_o, the Jacobian matrix (A.1) becomes

$$J(E_o) = \begin{bmatrix} 1 + ak_1 & 0 \\ 0 & 1 + ak_2 \end{bmatrix}. \tag{A.2}$$

It is quite obvious that (A.2) is a diagonal matrix and hence the corresponding eigenvalues are $\lambda_i = 1 + ak_i, i = 1, 2$ with eigenvectors (1, 0) and (0, 1). From the nonnegativity of the adjustment speed parameter, $k_i, i = 1, 2$ and from the auxiliary parameter a, it is clear that $|\lambda_i| > 1, i = 1, 2$, hence E_o is an unstable repelling node. □

Proof of Proposition 2. At E_1, the Jacobian matrix (A.1) becomes

$$J(E_1) = \begin{bmatrix} 1 - ak_1 & -\dfrac{k_1 ad}{2 + c_1} \\ 0 & 1 + ak_2\left(1 - \dfrac{d}{2 + c_1}\right) \end{bmatrix}. \tag{A.3}$$

It is clear that the matrix (A.3) is an upper triangular matrix whose eigenvalues are given by

$$\begin{aligned} \lambda_1 &= 1 - ak_1, \\ \lambda_2 &= 1 + ak_2\left(1 - \frac{d}{2 + c_1}\right). \end{aligned} \tag{A.4}$$

The corresponding eigenvectors are (1, 0) along the q_1 − axis and $(1, 1 - (k_1 d/k_1(2 + c_1) + k_2(2 + c_1 - d)))$, respectively. It is clear that $|\lambda_1| < 1$ gives $0 < k_1 < (2/a)$ and if $\lambda_2 > 1$, then E_1 is a saddle point. If $k_1 > (2/a)$, then E_1 is an unstable node. □

Proof of Proposition 3. The proof is similar to Proposition 2. □

Proof of Proposition 4. The Jacobian (A.1) at Nash point E_* becomes

$$J(E_*) = \begin{bmatrix} 1 - A(2 + c_1) & -Ad \\ -Bd & 1 - B(2 + c_2) \end{bmatrix}, \tag{A.5}$$

where

$$A = \frac{k_1 a(2 + c_2 - d)}{(c_1 + 2)(c_2 + 2) - d^2}, B = \frac{k_2 a(2 + c_1 - d)}{(c_1 + 2)(c_2 + 2) - d^2}, \tag{A.6}$$

and the trace τ and determinant δ are given by

$$\begin{aligned} \tau &= 2 - A(2 + c_1) - B(2 + c_2), \\ \delta &= AB\left((c_1 + 2)(c_2 + 2) - d^2\right) - B(2 + c_2) - A(2 + c_1) + 1. \end{aligned} \tag{A.7}$$

Using (A.6) and (A.7) Jury conditions, [30] can be obtained as follows:

$$1 - \tau + \delta = \frac{a^2(2 + c_1 - d)(2 + c_2 - d)}{(c_1 + 2)(c_2 + 2) - d^2} k_1 k_2, \tag{A.8a}$$

$$1 + \tau + \delta = 4 + \frac{a^2(2 + c_1 - d)(2 + c_2 - d)}{(c_1 + 2)(c_2 + 2) - d^2} k_1 k_2 - \frac{2a(c_1 + 2)(2 + c_2 - d)}{(c_1 + 2)(c_2 + 2) - d^2} k_1 - \frac{2a(c_2 + 2)(2 + c_1 - d)}{(c_1 + 2)(c_2 + 2) - d^2} k_2, \tag{A.8b}$$

$$1 - \delta = -\frac{a^2(2 + c_1 - d)(2 + c_2 - d)}{(c_1 + 2)(c_2 + 2) - d^2} k_1 k_2 + \frac{a(c_1 + 2)(2 + c_2 - d)}{(c_1 + 2)(c_2 + 2) - d^2} k_1 + \frac{a(c_2 + 2)(2 + c_1 - d)}{(c_1 + 2)(c_2 + 2) - d^2} k_2. \tag{A.8c}$$

Due to the nonnegativity of the auxiliary parameters a, c_1, c_2, and d, the condition (A.8a) is always positive. Simple calculations show that if the condition (A.8c) is greater than zero, this means that the condition (A.8b) is greater than zero and hence E_* is asymptotically stable. □

Proof of Proposition 5. Now, suppose that the condition (A.8b) is less than zero and the condition (A.8c) is kept nonnegative then using simple calculations, the point E_* loses its stability due to flip bifurcation if the following condition is achieved:

$$k_1 k_2 < \frac{(2 + c_1)}{a(2 + c_1 - d)} k_1 + \frac{(2 + c_2)}{a(2 + c_2 - d)} k_2 \tag{A.9}$$

□

Data Availability

The data used to support the findings of the study are included within the article.

Conflicts of Interest

The authors declare that they have no conflicts of interest.

Acknowledgments

This study was supported by the Researchers Supporting Project number (RSP2024R167), King Saud University, Riyadh, Saudi Arabia.

References

[1] T. Puu, "Chaos in duopoly pricing," *Chaos, Solitons and Fractals*, vol. 1, no. 6, pp. 573–581, 1991.

[2] C. H. Tremblay and V. J. Tremblay, "The Cournot-Bertrand model and the degree of product differentiation," *Economics Letters*, vol. 111, no. 3, pp. 233–235, 2011.

[3] D. Rand, "Exotic phenomena in games and duopoly models," *Journal of Mathematical Economics*, vol. 5, no. 2, pp. 173–184, 1978.

[4] J. Tuinstra, "A price adjustment process in a model of monopolistic competition," *International Game Theory Review*, vol. 06, no. 03, pp. 417–442, 2004.

[5] M. Ueda, "Effect of information asymmetry in Cournot duopoly game with bounded rationality," *Applied Mathematics and Computation*, vol. 362, Article ID 124535, 2019.

[6] N. Singh and X. Vives, "Price and quantity competition in a differentiated duopoly," *The RAND Journal of Economics*, vol. 15, no. 4, pp. 546–554, 1984.

[7] S. S. Askar and A. Al-khedhairi, "Dynamic investigations in a duopoly game with price competition based on relative profit and profit maximization," *Journal of Computational and Applied Mathematics*, vol. 367, Article ID 112464, 2020.

[8] S. S. Askar, "On Cournot–Bertrand competition with differentiated products," *Annals of Operations Research*, vol. 223, no. 1, pp. 81–93, 2014.

[9] S. S. Askar, "Tripoly Stackelberg game model: one leader versus two followers," *Applied Mathematics and Computation*, vol. 328, pp. 301–311, 2018.

[10] S. S. Askar and A. Al-Khedhairi, "Analysis of nonlinear duopoly games with product differentiation: stability, global dynamics, and control," *Discrete Dynamics in Nature and Society*, vol. 2017, pp. 1–13, 2017.

[11] S. Bylka and J. Komar, "Cournot-Bertrand mixed oligopolies," in *Warsaw Fall Seminars in Mathematical Economics 1975. Lecture Notes in Economics and Mathematical Systems*, M. Łoś, J. Łoś, and A. Wieczorek, Eds., Vol. 133, Springer, Berlin, Germany, 1976.

[12] J. Häckner, "A note on price and quantity competition in differentiated oligopolies," *Journal of Economic Theory*, vol. 93, no. 2, pp. 233–239, 2000.

[13] P. Zanchettin, "Differentiated duopoly with asymmetric costs," *Journal of Economics and Management Strategy*, vol. 15, no. 4, pp. 999–1015, 2006.

[14] A. Arya, B. Mittendorf, and D. E. M. Sappington, "Outsourcing, vertical integration, and price vs. quantity competition," *International Journal of Industrial Organization*, vol. 26, no. 1, pp. 1–16, 2008.

[15] A. A. Elsadany, "Dynamics of a Cournot duopoly game with bounded rationality based on relative profit maximization," *Applied Mathematics and Computation*, vol. 294, pp. 253–263, 2017.

[16] A. K. Naimzada and F. Tramontana, "Dynamic properties of a Cournot-Bertrand duopoly game with differentiated products," *Economic Modelling*, vol. 29, no. 4, pp. 1436–1439, 2012.

[17] J. Ma, L. Sun, S. Hou, and X. Zhan, "Complexity study on the Cournot-Bertrand mixed duopoly game model with market share preference," *Chaos*, vol. 28, no. 2, Article ID 023101, 2018.

[18] E. Ahmed, A. S. Hegazi, M. F. Elettreby, and S. S. Askar, "On multi-team games," *Physica A: Statistical Mechanics and its Applications*, vol. 369, no. 2, pp. 809–816, 2006.

[19] E. Ahmed and M. F. Elettreby, "Controls of the complex dynamics of a multi-market Cournot model," *Economic Modelling*, vol. 37, pp. 251–254, 2014.

[20] Y. Peng and Q. Lu, "Complex dynamics analysis for a duopoly Stackelberg game model with bounded rationality," *Applied Mathematics and Computation*, vol. 271, pp. 259–268, 2015.

[21] F. Tramontana, "Heterogeneous duopoly with isoelastic demand function," *Economic Modelling*, vol. 27, no. 1, pp. 350–357, 2010.

[22] J. Tanimoto, *Evolutionary Games with Sociophysics*, Springer, Berlin, Germany, 2019.

[23] J. Tanimoto, *Fundamentals of Evolutionary Game Theory and its Applications*, Springer, Berlin, Germany, 2015.

[24] J. Tanimoto, *Mathematical Analysis of Environmental System*, Springer, Berlin, Germany, 2014.

[25] W. Zhong, S. Kokubo, and J. Tanimoto, "How is the equilibrium of continuous strategy game different from that of discrete strategy game?" *Biosystems*, vol. 107, no. 2, pp. 88–94, 2012.

[26] S. Kokubo, Z. Wang, and J. Tanimoto, "Spatial reciprocity for discrete, continuous and mixed strategy setups," *Applied Mathematics and Computation*, vol. 259, pp. 552–568, 2015.

[27] H. Wang and J. Ma, "Complexity analysis of a Cournot-Bertrand duopoly game model with limited information," *Discrete Dynamics in Nature and Society*, vol. 2013, Article ID 287371, 6 pages, 2013.

[28] S. Brianzoni, L. Gori, and E. Michetti, "Dynamics of a Bertrand duopoly with differentiated products and nonlinear costs: analysis, comparisons and new evidences," *Chaos, Solitons and Fractals*, vol. 79, pp. 191–203, 2015.

[29] W. Zhou and H. Li, "Complex dynamical behaviors in a Bertrand game with service factor and differentiated products," *Nonlinear Dynamics*, vol. 106, no. 3, pp. 2739–2759, 2021.

[30] A. Al-Khedhairi, A. E. Matouk, and S. S. Askar, "Computations of synchronisation conditions in some fractional-order chaotic and hyperchaotic systems," *Pramana*, vol. 92, no. 5, p. 72, 2019.

[31] S. S. Askar, "A competition of duopoly game whose players are public: dynamic investigations," *Communications in Nonlinear Science and Numerical Simulation*, vol. 111, Article ID 106486, 2022.

[32] A. M. Awad, S. S. Askar, and A. A. Elsadany, "Complex dynamics investigations of a mixed Bertrand duopoly game: synchronization and global analysis," *Nonlinear Dynamics*, vol. 107, no. 4, pp. 3983–3999, 2022.

[33] B. Li, Y. Zhang, X. Li, Z. Eskandari, and Q. He, "Bifurcation analysis and complex dynamics of a Kopel triopoly model," *Journal of Computational and Applied Mathematics*, vol. 426, Article ID 115089, 2023.

[34] Z. Eskandari, Z. Avazzadeh, and R. Khoshsiar Ghaziani, "Complex dynamics of a Kaldor model of business cycle with discrete-time," *Chaos, Solitons and Fractals*, vol. 157, Article ID 111863, 2022.

[35] Z. Eskandari, J. Alidousti, and R. K. Ghaziani, "Codimension-one and-two bifurcations of a three-dimensional discrete game model," *International Journal of Bifurcation and Chaos*, vol. 31, no. 02, Article ID 2150023, 2021.

[36] Z. Wei, W. Tan, A. A. Elsadany, and I. Moroz, "Complexity and chaos control in a Cournot duopoly model based on bounded rationality and relative profit maximization," *Nonlinear Dynamics*, vol. 111, no. 18, pp. 17561–17589, 2023.

[37] G. Sarafopoulos and K. Papadopoulos, "Complexity and chaos control of A Cournot duopoly game with relative profit maximization and heterogeneous expectations," *KnE Social Sciences*, vol. 8, no. 1, pp. 172–193, 2023.

[38] V. Seralan, R. Vadivel, D. Chalishajar, and N. Gunasekaran, "Dynamical complexities and chaos control in a Ricker type predator-prey model with additive Allee effect," *AIMS Mathematics*, vol. 8, no. 10, pp. 22896–22923, 2023.

[39] S. Vinoth, R. Sivasamy, K. Sathiyanathan, B. Unyong, R. Vadivel, and N. Gunasekaran, "A novel discrete-time leslie–gower model with the impact of allee effect in predator population," *Complexity*, vol. 2022, Article ID 6931354, 21 pages, 2022.

[40] R. Vadivel, Z. T. Njitacke, L. Shanmugam, P. Hammachukiattikul, and N. Gunasekaran, "Dynamical analysis and reachable set estimation of T-S fuzzy system with permanent magnet synchronous motor," *Communications in Nonlinear Science and Numerical Simulation*, vol. 125, Article ID 107407, 2023.

[41] S. S. Askar and A. M. Alshamrani, "Cournot–bertrand duopoly model: dynamic analysis based on a computed cost," *Complexity*, vol. 2024, Article ID 5594918, 15 pages, 2024.

[42] L. Fanti, L. Gori, and M. Sodini, "Nonlinear dynamics in a Cournot duopoly with isoelastic demand," *Mathematics and Computers in Simulation*, vol. 108, pp. 129–143, 2015.

[43] G. I. Bischi, L. Stefanini, and L. Gardini, "Synchronization, intermittency and critical curves in a duopoly game," *Mathematics and Computers in Simulation*, vol. 44, no. 6, pp. 559–585, 1998.

[44] J. Alidousti, Z. Eskandari, and Z. Avazzadeh, "Generic and symmetric bifurcations analysis of a three dimensional economic model," *Chaos, Solitons and Fractals*, vol. 140, Article ID 110251, 2020.